On the Reduction of Wave Propagation Loss in Tunnels

Yoshio Yamaguchi, *Member, IEEE,* Takemitsu Honda, Masakazu Sengoku, *Member, IEEE,* Seiichi Motooka, and Takeo Abe, *Member, IEEE*

Abstract— **The reduction of radio wave attenuation in two-dimensional tunnels is discussed. The attenuation of the dominant mode due to its field penetration into the lossy dielectric side wall is reduced by means of the attachment of periodically aligned metallic strips on the wall surface. The electric field distribution in tunnels with and without strips are illustrated to show the effect on the attenuation characteristics. The efficiency of attenuation reduction rate by the metallic-wall stripping method is summarized. Finally, the calculation results based on the boundary element analysis is verified by a laboratory experiment.**

Key words— **tunnel, waveguide, attenuation, propagation loss, boundary element method.**

I. Introduction

With the rapid development of radio communications including cellular communication, wire-less communication and portable communication, the radio waves in the frequency range from HF to microwave bands are now densely utilized everywhere. However, the attenuation of the radio wave in tunnels, buildings, underground streets, and parking lots in basements, poses adverse problems for these radio wave communications. It is well known that low frequency signals such as "radio broadcasting or VHF amateur radio" cannot be heard in tunnels. This is due to the cut-off propagation or the large attenuation of the wave.

Here we focus our attention to the attenuation characteristics in tunnels including corridors and underground streets. In general, the tunnels may be considered as hollow waveguides surrounded by lossy materials. Many theoretical and experimental studies on the propagation characteristics have been carried out including fundamental propagation characteristics [1]–[13], excitation [14]–[17], field distribution [18]–[22], and effect of obstacles [18]–[20]. From extensive research investigations of the tunnel problem, the results on straight tunnel propagation can be summarized as follows:

1) From an analytical point of view, tunnels are waveguides of arbitrary cross section surrounded by lossy dielectric materials.
2) The attenuation constant is due to refraction loss and ohmic loss in the surrounding walls whose dielectric properties vary with frequency. Typical frequency characteristics of attenuation constant are shown in Fig. 1.
3) The refraction loss plays a dominant role in the attenuation characteristics at higher frequencies where the wavelength is much smaller than the cross-sectional dimension, because the surrounding material acts as a pure dielectric at frequencies above the UHF band. There exists a high number of modes in tunnels in this higher frequency region; however, the lowest attenuated mode is the dominant mode whose attenuation constant is inversely proportional to the frequency squared and to the cubic size of the cross-sectional dimension. These characteristics correspond to region A in Fig. 1. This dominant mode is the hybrid mode in nature in an actual tunnel and corresponds to the TE_{10} mode in a metallic rectangular waveguide.
4) The ohmic loss plays a dominant role at lower frequencies when the wavelength is comparable with the tunnel dimension because the surrounding material then tends to act as a heavily lossy dielectric as the electromagnetic field penetrates into the surrounding medium resulting in the ohmic loss. This characteristic corresponds to region B in Fig. 1.
5) There exists a vague cut-off frequency according to the dimensional size of the tunnel cross section. The value is not apparent as for the case of a metallic waveguide, because the attenuation continuously and gradually increases as the frequency decreases for the lossy case (region C in Fig. 1).

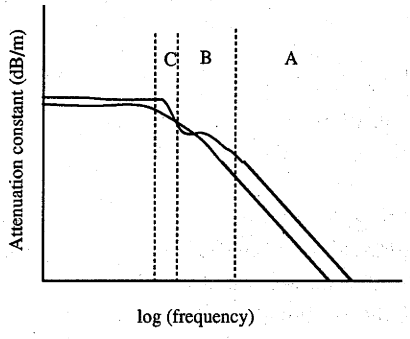

Fig. 1. Typical frequency characteristics of attenuation constants.

It is important to reduce attenuation in these structures. However, only a few research studies [23], [24] on the reduction of attenuation in tunnels have been carried out to expand the radio communications capability and to utilize

Manuscript received June 3, 1991; revised November 18, 1991. This work was supported in part by the Telecommunications Advancement Foundation.

Y. Yamaguchi, T. Honda, and M. Sengoku are with the Department of Information Engineering, Faculty of Engineering, Niigata University, Ikarashi 2-8050, Niigata-shi 950-21, Japan.

S. Motooka and T. Abe are with the Department of Electronics Engineering, Chiba Institute of Technology, Narashino 2-17-1, Chiba 275, Japan.

IEEE Log Number 9106271.

it. Here, in this analysis, we propose one method to reduce the attenuation in tunnels. From the outset, we know that in the higher frequency region where the wavelength is much smaller than the tunnel dimension the attenuation is very small, for which the reduction is less important. However, in the lower frequency region where the wavelength is close to the tunnel dimension, we still encounter the propagation mode with large attenuation. It is our purpose to reduce the attenuation constant of the dominant mode in this frequency region. The main factor that contributes to the attenuation in this frequency region is the penetration of the electromagnetic field into the surrounding material which results in the ohmic loss. Hence, the basic idea to reduce the attenuation is to limit the penetration of the field into the lossy walls, which leads to the use of some metallic material on the tunnel walls for shielding purposes.

The shielding techniques may consist of using metallic strips, geometrical combination of strips, or wire nettings. Among them, the fine wire-nettings is the most efficient for the reduction of the propogation loss for which we have already reported the efficiency based on a laboratory experiment [24]. However, it still needs analytical investigations including the formulation of mesh shape and size with respect to the wavelength into consideration. The analysis is extremely difficult at present. On the other hand, an insulated wire along a tunnel, although it is not in the category of shielding, may be considered to work well for the reduction of the loss. The wire must be put close to tunnel wall so as not to disturb traffic in tunnels. From a laboratory experiment, the insulated wire close to tunnel wall causes additional loss in the frequency considered here because the propagation mode changes from the dominant mode to a quasi-TEM mode. The insulated wire works well in the cut-off frequency region [25]. Upon these considerations, we investigated analytically and experimentally how much the attenuation could be reduced in tunnels using metallic strips on side walls. In the following, a brief analytical formulation based on the boundary element method is outlined. Then the effects of the metallic strips placed on the side walls are examined by computer simulation illustrating the field distribution in tunnels. A laboratory experiment is carried out to show the validity of this method. Finally, the efficiency of reduction by the metallic-wall stripping method is summarized.

II. Formulation

Consider the two-dimensional tunnel as shown in Fig. 2. The field in the tunnel has no variations in the y direction. This two-dimensional tunnel is realized by covering the ceiling and the bottom with two parallel perfectly conducting plates with small spacing with respect to the wavelength. The reason why we consider the two-dimensional tunnel is: 1) the effect of metallic strip on the propagation loss can be obtained, 2) the analysis becomes simpler than that in the three-dimensional case including computer simulation because the three-dimensional analysis demands formidable task.

At first, we examine the field distribution of the dominant mode by the boundary element method [21], [22]. In order

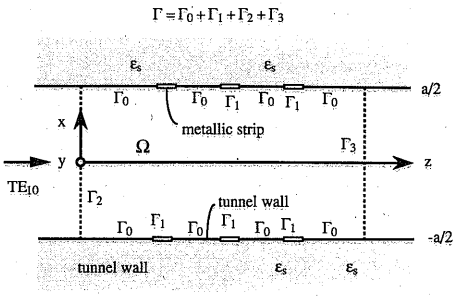

Fig. 2. Plane view of two-dimensional tunnel and the boundary Γ.

to simplify the analysis, we assume that the TE_{10} wave, the dominant mode in this structure, is incident from the z-direction. At $z = 0$, the wave is launched into the region where we are concerned.

If we let the dominant electric field component E_y be u, the wave equation

$$\frac{\partial^2 u}{\partial x^2} + \frac{\partial^2 u}{\partial z^2} + k_0^2 u = 0 \tag{1}$$

holds in this two-dimensional structure, where

$$k_0 = \omega\sqrt{\varepsilon_0\mu_0} = \frac{2\pi}{\lambda}, \tag{2}$$

ω: angular frequency,

λ: wavelength in free space,

ε_0: permittivity of free space,

μ_0: permeability of free space.

We divide the boundary Γ for this structure into Γ_0 (lossy side walls), Γ_1 (metallic strip walls), Γ_2 (hypothetical entrance), and Γ_3 (hypothetical exit) as shown in Fig. 2. If we let u^* be the two-dimensional scalar Green's function for unbounded region, then we obtain the following equation for the boundary element analysis

$$c_i u_i + \int_\Gamma q^* u \, d\Gamma = \int_\Gamma u^* q \, d\Gamma \tag{3}$$

where u_i is the value of u at the observation point, and q is the derivative of u with respect to the normal direction $\mathbf{n}$ of the boundary (See Fig. 3). The coefficient c_i is unity in the interior region, while the value on the boundary is determined by the angle made by the two adjacent boundary elements. Since we are dealing with the two-dimensional structure, the Green's function u^* and its normal derivative q^* can be written as

$$u^* = -\frac{j}{4} H_0^{(2)}(k_0 r) \tag{4}$$

$$q^* = \frac{\partial u^*}{\partial n} = -\frac{j}{4} k_0 H_1^{(2)}(k_0 r)\cos\phi \tag{5}$$

where $H_0^{(2)}$ and $H_1^{(2)}$ are the Hankel functions of the second kind of order 0 and 1, respectively; r is the magnitude of vector $\mathbf{r}$ from the point i to a point on the boundary indicating

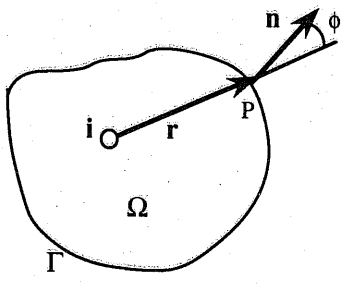

Fig. 3. Region Ω surrounded by boundary Γ.

the distance, and ϕ is the angle sustained by the vector $\mathbf{r}$ and the normal vector $\mathbf{n}$ on the boundary as shown in Fig. 3.

We divide each boundary into line elements and discretize the integral (3). With unknown function u and q expressed by polynomial interpolation function, (3) can be rewritten in a set of linear algebraic equations

$$c_i u_i + \sum_{j=1}^{n} H_{ij} u_j = \sum_{j=1}^{n} G_{ij} q_j \tag{6}$$

where n is the total number of nodal points. The interpolation function used here is the Lagrangian interpolation function with one-dimensional, three-noded elements which is the second-order polynomials as in [26]. These equations (6) can be combined together and be written in a matrix form as

$$[H]\{u\} = [G]\{q\} \tag{7}$$

which enables us to solve it if u or q, or the relation between u and q on the boundary Γ is specified. In the following we adopt boundary conditions and an analysis similar to that presented by Sakai and Koshiba [21], [22]. The boundary conditions for this problem are the same as those presented in [21] except for the metallic portion Γ_1.

A. Boundary Condition for the Wall Sections Γ_0 and Γ_1

The boundary on the side wall consists of Γ_0 and Γ_1. The boundary condition for this mode is the continuity of tangential components (E_y and H_z). This condition can be satisfied by matching the impedances at side surface walls. To this purpose, we employ the same technique proposed in [10], [23], i.e., the surface impedance method presented by Yasumoto [10] as below

$$E_y = \pm Z_s H_z \quad \left(x = \pm \frac{a}{2}\right). \tag{8}$$

The surface impedance for this mode is given by Sakai [21]

$$Z_s = \frac{Z_0}{\sqrt{\varepsilon_s - \sin^2\theta}}, \quad Z_0 = \sqrt{\frac{\mu_0}{\varepsilon_0}} \tag{9}$$

$$\varepsilon_s = \frac{\varepsilon}{\varepsilon_0} - j\frac{\sigma}{\omega\varepsilon_0} = \varepsilon_r - j\varepsilon_i \tag{10}$$

where ε_s is the relative permittivity and σ is the conductivity of the side wall, θ is the incident angle of the plane wave which impinges on the side wall.

After having determined the relation among the field components of $\mathbf{E}$ and $\mathbf{H}$, we obtain the relation for the boundary element analysis as follows:

$$q = -jk_0\sqrt{\varepsilon_s - \sin^2\theta}\, u. \tag{11}$$

For the boundary section Γ_1, the electric field vanishes on the metallic strip. Hence, u is equal to zero on Γ_1 from the outset.

B. Boundary Condition for the Hypothetical Boundary Γ_2 and Γ_3 (Entrance and Exit)

The field in the tunnel can be expanded as a sum of lossy propagation modes. This field expression is matched to the incident TE_{10} mode at the entrance of $z = 0$. This matching operation combines the internal numerical solution to the exterior analytical solution. Thus, the boundary condition for Γ_2 can be given as

$$\{q\}_2 = \left(\gamma_2 + [F]_2[\gamma]_2[F]_2^{-1}\right)\{f\}_2 - \left([F]_2[\gamma]_2[F]_2^{-1}\right)\{u\}_2 \tag{12}$$

where $\{u\}_2$ and $\{q\}_2$ are row vectors consisting of values on Γ_2, while $[F]_2$ is the matrix

$$[F]_2 = \begin{bmatrix} f_1\left(x_1^{(2)}\right) & f_2\left(x_1^{(2)}\right) & \cdots & f_{n1}\left(x_1^{(2)}\right) \\ f_1\left(x_2^{(2)}\right) & f_2\left(x_2^{(2)}\right) & \cdots & f_{n1}\left(x_2^{(2)}\right) \\ \vdots & \vdots & \ddots & \vdots \\ f_1\left(x_{n1}^{(2)}\right) & f_2\left(x_{n1}^{(2)}\right) & \cdots & f_{n1}\left(x_{n1}^{(2)}\right) \end{bmatrix} \tag{13}$$

composed of

$$f_m\left(x^{(2)}\right) = \begin{cases} \cos k_m x^{(2)} & (m:\ \text{odd}) \\ \sin k_m x^{(2)} & (m:\ \text{even}). \end{cases} \tag{14}$$

The first term in right-hand side of (12) corresponds to incident wave and the second term corresponds to reflected wave. The row vector $\{f\}_2$ is of the following form:

$$\{f\}_2 = \left[f_2\left(x_1^{(2)}\right), f_2\left(x_2^{(2)}\right), \cdots, f_2\left(x_{n1}^{(2)}\right)\right]^T \tag{15}$$

where T denotes transpose, $x_1^{(2)}, x_2^{(2)}, \cdots, x_{n1}^{(2)}$ are the coordinates of the nodal points on Γ_2, and $[\gamma_2]$ is given by the diagonal matrix

$$[\gamma]_2 = \begin{bmatrix} \gamma_1 & 0 & \cdots & 0 \\ 0 & \gamma_2 & \cdots & 0 \\ \vdots & \vdots & \ddots & \vdots \\ 0 & 0 & \cdots & \gamma_{n1} \end{bmatrix} \tag{16}$$

with elements

$$\gamma_m = \sqrt{k_m^2 - k_0^2} = \alpha_m + j\beta_m \tag{17}$$

α_m: attenuation constant, β_m: phase constant,

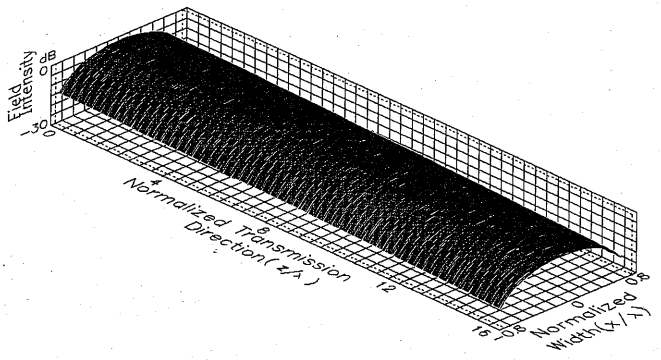

Fig. 4. Field pattern in hollow tunnel.

which are the solutions of the characteristic equations derived from the transverse resonance technique [21], [23]

$$k_m \tan \frac{k_m a}{2} = jk_0\sqrt{\varepsilon_s - \sin^2\theta} \quad (m: \text{odd}),$$
$$k_m \cot \frac{k_m a}{2} = -jk_0\sqrt{\varepsilon_s - \sin^2\theta} \quad (m: \text{even}). \quad (18)$$

For the exit of the tunnel boundary Γ_3, we assume that there does not exist a returned wave (i.e., no incoming wave into the region). Thus, the boundary condition can be written as

$$\{q\}_3 = -\left([F]_3[\gamma]_3[F]_3^{-1}\right)\{u\}_3 \quad (19)$$

where each vector and matrix are the same as those for the entrance except that the corresponding values are computed on the boundary Γ_3.

After having determined u and q on all boundary $\Gamma = \Gamma_0 + \Gamma_1 + \Gamma_2 + \Gamma_3$, one can obtain the field strength u in the interior region using

$$u_i = \sum_{k=1}^{m} \int_{\Gamma_k} (qu^* - uq^*)\, d\Gamma. \quad (20)$$

III. Hollow Tunnel

We carried out a computer simulation for a hollow tunnel to show the property of the dominant mode including the field distribution and the attenuation constant in comparison with an analytical solution. We first determine the electric field distribution in a tunnel without strips because it is the fundamental one which we are dealing with. In this calculation, the boundary condition for Γ_0 is employed instead of the condition for Γ_1 on the place where the strips are located. The parameters chosen in the calculation are:

width of the tunnel : $a = 1.6\lambda$

complex permittivity of the wall : $\varepsilon_s = \varepsilon_r - j\varepsilon_i = 5 - j$.

Fig. 4 shows the three-dimensional display of the electric field distribution (E_y) in the region from $z = 0$ to $z = 16\lambda$. The values are normalized at the entrance of the tunnel (i.e., a unit magnitude TE_{10} mode is incident at $z = 0$). In the calculation, the interval of the nodal point is taken less than $\lambda/10$. The total number of the nodal points along the boundary is chosen to be 358. One can see that the whole pattern is also close to the measured one [20] which has been measured in a three-dimensional tunnel. The pattern is then cut in the transverse direction, which results in the cross-sectional distribution in the hollow tunnel. Fig. 5 shows the calculated patterns evaluated at $z = 0$ which are close to a cosine distribution of the dominant mode. It can be seen that the electric field at the side wall boundary increases as the real permittivity decreases which results in large absorption of power in tunnel wall.

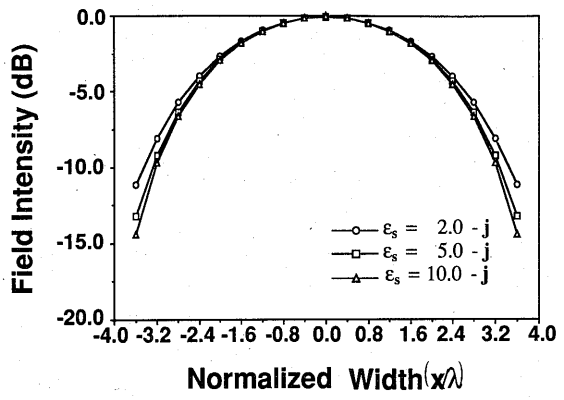

Fig. 5. Field distribution in the transverse direction.

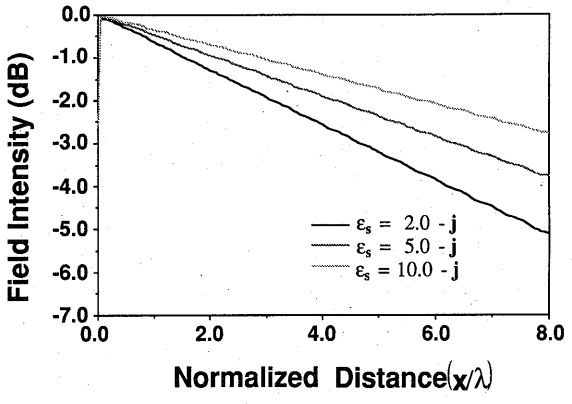

Fig. 6. Field strength as a function of normalized transmission distance along the center line of tunnel.

Fig. 6 shows longitudinal cut view of the field pattern (Fig. 4) along the center line of the tunnel. The magnitude of the electric field in decibels decreases linearly with transmission distance, providing the attenuation constant. It is possible to determine the attenuation constant from this slope straightforwardly. The attenuation constants per wavelength λ are calculated in Table I as a function of permittivity and are compared with an analytical solution of (18) with $m = 1$ and $\theta = 72°$ (also refer to [2]). There is a good agreement between this numerical method and the analytical one. As the permittivity increases, the attenuation decreases. This is due to the impedance difference at the tunnel wall, i.e., if the impedance difference becomes larger, then the field does not penetrate easily into the wall, which results in low attenuation.

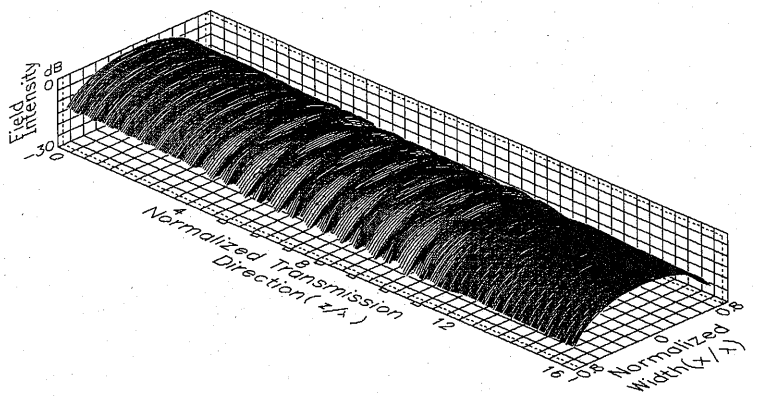

(a)

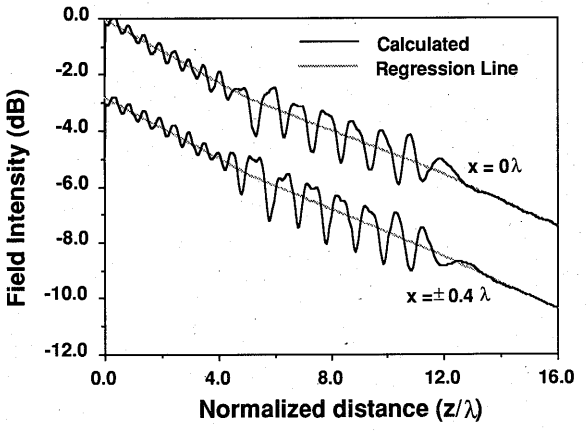

(b)

Fig. 7. Field pattern in tunnel with strips placed on side walls, (a) strip width $\delta = 0.2\lambda$ (b) longitudinal cut-views at $x = 0$ and $x = \pm 0.4$.

TABLE I
ATTENUATION PER WAVELENGTH (dB/λ)

ε_r	boundary element method	analytical method
$2.0 - j1.0$	0.682094	0.684533
$3.0 - j1.0$	0.635385	0.633491
$4.0 - j1.0$	0.568122	0.565967
$5.0 - j1.0$	0.512694	0.510838
$6.0 - j1.0$	0.469017	0.467458
$7.0 - j1.0$	0.434139	0.432812
$8.0 - j1.0$	0.405681	0.404532
$9.0 - j1.0$	0.381983	0.380970
$10.0 - j1.0$	0.361890	0.360989

IV. REDUCTION OF PROPAGATION LOSS

Incorporating the boundary condition that the electric field vanishes on the metallic surface of the strips, the field strength in the tunnel now can be analyzed to examine the effect of strips on the propagation problem. In the calculation, the total number of the nodal points is chosen to be 482 on the whole boundary Γ which includes 322 points on the boundary Γ_0, 126 points on the boundary Γ_1, 17 points on the boundary Γ_2, and 17 points on the boundary Γ_3. The allocation interval of the nodal points is less than $\lambda/10$ along the boundaries. The tunnel parameters are:

$$\text{permittivity } \varepsilon_s = \varepsilon_r - j\varepsilon_i = 5 - j,$$
$$\text{tunnel width } a = 1.6\lambda, \text{ strip width } \delta = 0.2\lambda,$$
$$\text{number of strips} = 7, \text{ period } p = \lambda.$$

The field distribution in the tunnel is shown in Fig. 7(a) where the positions of strips are indicated by small rectangular boxes. The pattern is not so smooth as those in hollow tunnels due to standing wave phenomenon created by strips. As can be seen from this figure, the field strength near the strips becomes smaller compared to the field near the lossy wall. Apparently, this is due to the metallic wall, however, one can anticipate that the field does not penetrate into the surrounding wall due to strips. This fact indicates that the attenuation of the wave may be reduced by these strips. In order to examine the effect on the propagation characteristics, we made cut-views along the center line (at $x = 0$) and a gangway (at $x = \pm 0.4$) of the tunnel which are shown in Fig. 7(b). In this figure, the regression lines to the regions with and without strips are shown for the sake of comparison. One can see that the slope of the line (attenuation constant) in the region with strip is flatter than that in the other regions without strip. In other words, the attenuation constant is reduced by an attachment

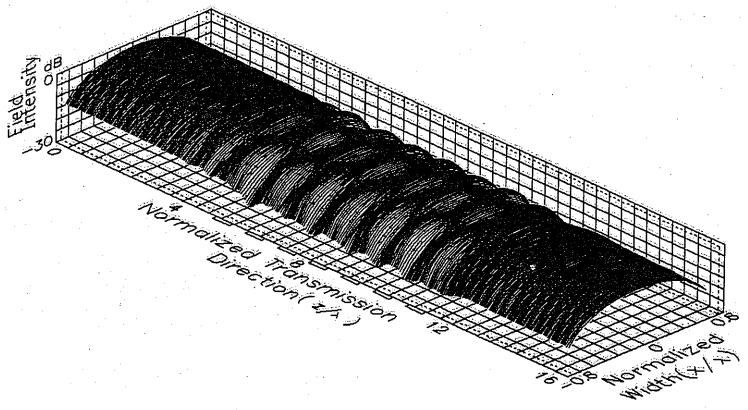

(a)

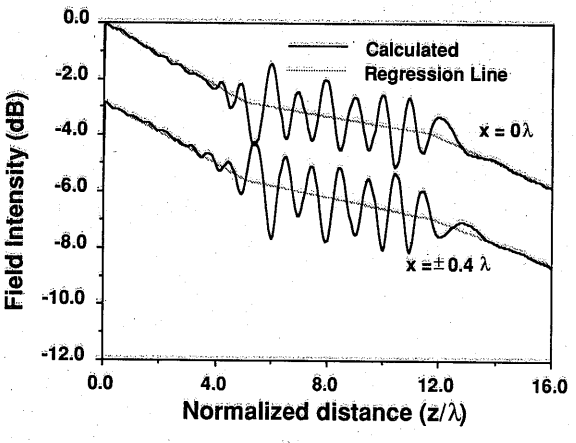

(b)

Fig. 8. Field pattern in tunnel with strips placed on side walls, (a) strip width $\delta = 0.5\lambda$ (b) longitudinal cut views at $x = 0$ and $x = \pm 0.4$.

of these strips. Thus it is possible to reduce the attenuation constant by this method.

Another calculated example for $\delta = 0.5\lambda$ is shown in Fig. 8. The pattern in the tunnel is slightly different from that in Fig. 7. The standing pattern depends mainly on strip width. The variation of the electric field intensity due to strips in the order of several decibels seen in Fig. 7(b) and Fig. 8(b) does not cause fading effect in radio communications, however, the smaller, the better.

There is a high number of parameters such as strip width, interval, location including periodic or random positioning to determine the effect of strips on the attenuation characteristics. Thus, we use a simple parameter s for the evaluation

$$s = \delta/p \quad (0 < s < 1) \tag{21}$$

where δ is the width of strip and p is the periodic strip interval. The reason for choosing this parameter is such that if the side walls are fully covered with metal, then the attenuation is approximately zero; on the other hand, if there is no strip on the wall, the attenuation becomes that of the hollow tunnel. It can be anticipated that the attenuation varies with the area percentage of strip. That is, if we add strips, the attenuation reduction rate should increase in proportion to the area that we add. We carried out some calculations on the field distribution similar to Figs. 7 and 8, and examined the efficiency of strips on the reduction of the attenuation constant based on this idea. The final result is shown in Fig. 9 where the vertical axis is measured by the ratio of the attenuation constant α_s in tunnels with strip to α_0 in tunnels without strip, while the horizontal axis is measured by the percentage parameter $s = \delta/p$. For the sake of comparison, the criteria line of an approximate formula

$$\frac{\alpha_s}{\alpha_0} = 1 - \frac{\delta}{p} = 1 - s$$

is drawn together in Fig. 9. It is seen that the ratio of the attenuation constant α_s/α_0 is smaller than $1 - s$. This is practically an important result, because the attenuation reduction by such strips is larger than the expectation. This reduction rate becomes larger in narrower tunnels and the low attenuation transmission is achieved in the narrower tunnel (i.e., in the lower frequency) where the absolute attenuation is large.

V. Laboratory Experiment

In order to confirm these theoretical results, we carried out a laboratory measurement on attenuation constant. Fig. 10 shows the block diagram of the measurement scheme. Using a spectrum analyzer, we measured the field strength in a two-dimensional tunnel which consisted of two concrete blocks and

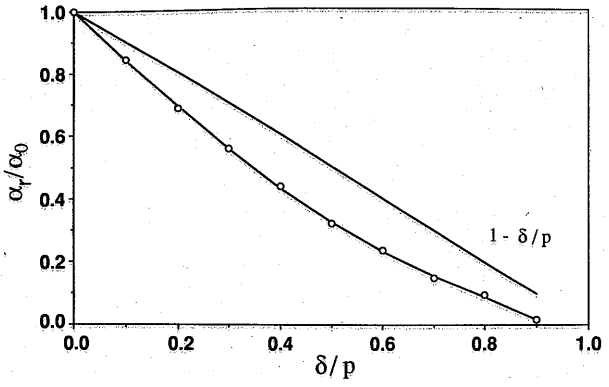

Fig. 9. Ratio of attenuation constant α_s/α_0 as a function of δ/p.

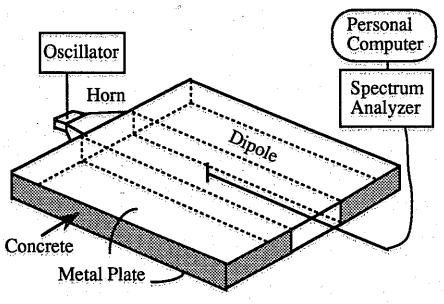

Fig. 10. Measurement scheme.

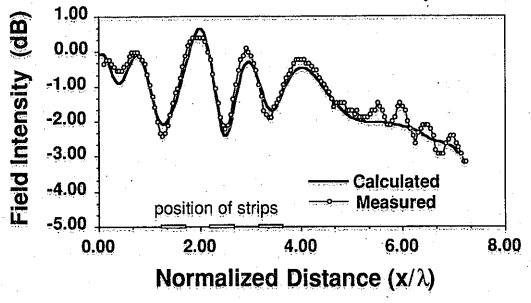

(a)

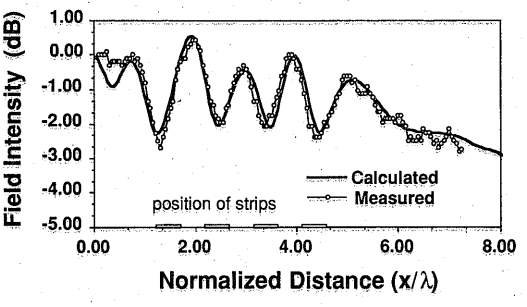

(b)

Fig. 11. Experimental and calculated field strength along the tunnel, (a) three strips, and (b) four strips.

two metallic plates. The tunnel size is 8 cm in width ($= 1.6\lambda$), 5 cm in height, and 100 cm in length. The number of strips employed in this tunnel is 3 and 4. The operating frequency is 6 GHz. The field strength along the center line of the tunnel was picked up by a small dipole antenna. The results are shown in Fig. 11 where the calculated patterns are also illustrated. We notice that the experimental results show a good agreement between the measured value and the calculated one.

VI. Concluding Remarks

Based on the boundary element analysis, a technique for the reduction of the attenuation constant for the dominant mode in two-dimensional tunnels has been presented. The electromagnetic field penetration into the surrounding wall is reduced by metallic strips placed on the walls, which leads to a reduction of the propagation loss. The attachment of strips is particularly effective for the lower frequency region where the wavelength and tunnel dimension are comparable.

The experimental results in two-dimensional tunnel is in a good agreement with the calculated ones. The detailed characteristics of the propagation mode can now be made available by computer simulations. Thus, the most effective positioning of strips and the best way to utilize these strips is now being investigated and will be reported in the future.

Acknowledgment

The authors are grateful to Professor Wolfgang -M. Boerner at the University of Illinois at Chicago for the revision of the manuscript.

References

[1] S.F. Mahmoud and J.R. Wait, "Geometrical optical approach for electromagnetic propagation in rectangular mine tunnels," *Radio Sci.*, vol. 9, no. 12, pp. 1147–1158, 1974.

[2] A.G. Emslie, L.L. Robert, and P.F. Strong, "Theory of the propagation of UHF radio waves in coal mine tunnels," *IEEE Trans. Antennas Propagat.*, vol. AP-23, no. 2, pp. 192–205, Mar. 1975.

[3] J. Chiba, T. Inaba, Y. Kuwamoto, O. Banno, and R. Sato, "Radio communication in tunnels," *IEEE Trans. Microwave Theory Tech.*, vol. MTT-26, no. 6, pp. 439–443, June 1978.

[4] Y. Yamaguchi, T. Abe, and T. Sekiguchi, "Propagation characteristics of normal modes in hollow circular cylinder surrounded by dissipative medium," *Trans. IECE Japan*, vol. 62-B, no. 4, pp. 368–373, 1979.

[5] S. Kozono, T. Suzuki, and T. Hanazawa, "Experimental study of mobile radio propagation characteristics in rectangular tunnels," *Trans. IECE Japan*, vol. J62-B, no. 6, pp. 565–572, June 1979.

[6] Y. Yamaguchi, T. Abe, and M. Tsuchida, "Propagation constant in hollow circular cylinder surrounded by two lossy layers," *Trans. IECE Japan*, vol. J64-B, no. 4, pp. 312–317, Apr. 1981.

[7] T. Abe and Y. Yamaguchi, "Propagation constant below cut-off frequency in a circular waveguide with conducting medium," *IEEE Trans. Microwave Theory Tech.*, vol. MTT-29, no. 7, pp. 707–712, July 1981.

[8] Y. Yamaguchi, T. Simizu, and T. Abe, "Propagation characteristics of the dominant mode in tunnels with elliptical cross section," *Trans. IECE Japan*, vol. J64-B, no. 9, pp. 1032–1038, Sept. 1981.

[9] Y. Yamaguchi, T. Abe, and T. Sekiguchi, "Propagation characteristics of the dominant mode in tunnels," *Trans. IECE Japan*, vol. J65-B, no. 4, pp. 471–476, Apr. 1982.

[10] K. Yasumoto and H. Shigematsu, "Analysis of propagation characteristics of radio waves in tunnels using surface impedance approximation," *Radio Sci.*, vol. 19, no. 2, pp. 597–602, 1984.

[11] B. Jacard and O. Maldonado, "Microwave modeling of rectangular tunnels," *IEEE Trans. Microwave Theory Tech.*, vol. MTT-32, pp. 576–581, 1984.

[12] Y. Yamaguchi, T. Abe, T. Sekiguchi, and J. Chiba, "Attenuation constants of UHF radio waves in arched tunnels," *IEEE Trans. Microwave Theory Tech.*, vol. MTT-33, no. 8, pp. 714–718, Aug. 1985.

[13] Y. Yamaguchi and T. Abe, "Attenuation characteristics of radio waves in rectangular tunnels by reflection coefficient," *Trans. IECE Japan*, vol. J66-B, no. 12, pp. 1518–1519, Dec. 1983.

[14] K. Uchida, T. Matsunaga, K. Yoshidomi, and K. Aoki, "Electromagnetic wave excitation in a two-dimensional tunnel by waveguide modes," *Trans. IECE Japan*, E68, no. 3, pp. 159–165, Mar. 1985.

[15] K. Uchida, T. Matsunaga, and T. Noda, "Electromagnetic wave excitation in a two-dimensional impedance tunnel with a cross-junction," *Trans. IEICE Japan,* E70, no. 7, pp. 634–639, July 1987.
[16] T. Matsunaga, K. Uchida, and T. Noda, "Electromagnetic wave propagation in a two-dimensional tunnel," *Trans. IEICE Japan,* vol. J72-B-II, no. 1, pp. 26–33, Jan. 1989.
[17] T. Matsunaga, K. Uchida, and T. Noda, "Electromagnetic wave propagation in a two-dimensional tunnels with modified multi-cross-junctions," *Trans. IEICE Japan,* vol. J72-B-II, no. 8, pp. 390–395, Aug. 1989.
[18] Y. Yamaguchi, T. Abe, and T. Sekiguchi, "Experimental study of radio propagation characteristics in an underground street and corridors," *IEEE Trans. Electromagnet. Compat.,* vol. EMC-28, no. 3, pp. 148–155, Aug. 1986.
[19] Y. Yamaguchi, T. Abe, and T. Sekiguchi, "Radio propagation characteristics in underground streets crowded with pedestrians," *IEEE Trans. Electromagnet. Compat.,* vol. 30, no. 2, pp. 130–1136, May 1988.
[20] Y. Yamaguchi, T. Abe, and T. Sekiguchi, "Radio propagation loss in the VHF to Microwave region due to vehicles in tunnels," *IEEE Trans. Electromagnet. Compat.,* vol. 31, no. 1, pp. 87–91, Feb. 1989.
[21] K. Sakai and M. Koshiba, "Application of the boundary-element method to an infinitely long tunnel," *Trans. IEICE Japan,* vol. J-71-B, no. 7, pp. 872–881, 1988.
[22] K. Sakai and M. Koshiba, "Analysis of electromagnetic field distribution in tunnels with partition walls," *Trans. IEICE Japan,* vol. J72-B-II, no. 11, pp. 595–602, 1989.
[23] Y. Yamaguchi, T. Abe, and T. Sekiguchi, "Improvement of attenuation characteristics in tunnels (I)," *Tech. Rep, of IECE,* A-P 83-11, May 1983.
[24] Y. Yamaguchi, T. Abe, and T. Sekiguchi, "Improvement of attenuation characteristics in tunnels (II)," *Tech. Rep. of IECE,* EMCJ 83-48, Oct. 1983.
[25] J. R. Wait, *Electromagnetic Wave Theory.* New York: Harper & Row, 1985, pp. 213–219.
[26] M. V. K. Chari and P. P. Silvester, *Finite Elements in Electrical and Magnetic Field Problems.* New York: Wiley, 1980, pp. 53–56.

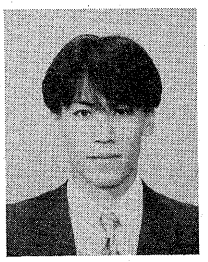

Takemitsu Honda was born in Fukushima, Japan, on January 30, 1969. He received the B.E. degree from Niigata University, Japan, in 1991. He is now a graduate student pursuing the Master's degree at Niigata University working with boundary element analysis in electromagnetic problem.

Mr. Honda is an associate member of the Institute of Electronics, Information and Communication Engineers of Japan.

Masakazu Sengoku (S'70–M'72) photograph and biography not available at the time of publication.

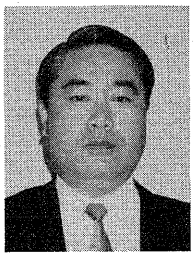

Seiichi Motooka was born in Hiroshima, Japan, on January 14, 1940. He received the B.S. degree in electric engineering from Chiba Institute of Technology, Chiba, Japan, in 1963 and the Dr. Eng. degree in applied electronics from Tokyo Institute of Technology, Yokohama, Japan.

He has been a Professor at the Department of Electronics, Chiba Institute of Technology since 1983, working in the Underground Tomography by using Electromagnetic Wave and Impulsive Sound, Measurement of Underwater Acoustics and Non-destructive Testing using Impulsive Sound.

Dr. Motooka is a member of the Institute of Electronics, Information and Communication Engineers of Japan, the Institute of Electrical Engineers of Japan, and the Acoustical Society of Japan.

Yoshio Yamaguchi (M'81) photograph and biography not available at the time of publication.

Takeo Abe (M'79) photograph and biography not available at the time of publication.